Theoretical Study of the Structural and Spectroscopic Properties of Stellacyanin

Jan O. A. De Kerpel and Kristine Pierloot*

Department of Chemistry, University of Leuven, Celestijnenlaan 200F, B-3001 Heverlee-Leuven, Belgium

Ulf Ryde and Björn O. Roos

Department of Theoretical Chemistry, Chemical Center, P.O. Box 124, S-221 00 Lund, Sweden

Received: December 8, 1997; In Final Form: March 6, 1998

The electronic spectrum of the azurin Met121Gln mutant, a model of the blue copper protein stellacyanin, has been studied by ab initio multiconfigurational second-order perturbation theory (the CASPT2 method), including the effect of the protein and solvent by point charges. The six lowest electronic transitions have been calculated and assigned with an error of less than 2400 cm^{-1}. The ground-state singly occupied orbital is found to be a predominantly π antibonding orbital involving Cu3d and $S_{cys}3p_{\pi}$. However, it also contains a significant amount (18%) of $Cu-S_{cys}$ σ antibonding character. This σ interaction is responsible for the appearance in the absorption spectrum of a band at 460 nm, with a significantly higher intensity than observed for other, axial, type 1 copper proteins (i.e., plastocyanin or azurin). The $\pi-\sigma$ mixing is caused by the axial glutamine ligand binding at a much shorter distance to copper than the corresponding methionine ligand in the normal blue copper proteins. This explains why, based on its spectral properties, stellacyanin is classified among the rhombic type 1 copper proteins, although its structure is clearly trigonal, as it is for the axial proteins. Calculations have also been performed on structures where the glutamine model coordinates to the copper ion via the deprotonated N^{ϵ} atom instead of the O^{ϵ} atom. However, the resulting transition energies do not resemble the experimental spectrum obtained at normal or elevated pH. Thus, the results do not confirm the suggestion that the coordinating atom of glutamine changes at high pH.

Introduction

Oxidized blue copper proteins exhibit a number of extraordinary characteristics that distinguish them from small inorganic Cu(II) complexes[1,2] (e.g., an intense absorption band around 600 nm (the blue band), a low electron paramagnetic resonance hyperfine coupling constant, and a high redox potential). The active site of these proteins contains a single copper ion, surrounded in an almost planar fashion by three strongly bound ligands: the N^{δ} atoms of two histidine residues and the S^{γ} atom of a cysteine residue. A fourth ligand is axial to this plane, usually a S^{δ} atom of methionine.

On the basis of copper ligand surrounding, the blue copper proteins have been divided into four groups.[3] The first group consists of the classical blue copper site as it is found in plastocyanin, for example, with the four ligands as described above. The second group comprises the azurins, which have an additional carbonyl oxygen ligand trans to the axial methionine ligand. The third group contains the perturbed blue copper sites (i.e., pseudoazurin, cucumber basic protein, and the type 1 copper center in nitrite reductase), which have the same four ligands as the first class, but a significantly shorter $Cu-S_{Met}$ bond length. The fourth group contains blue copper proteins in which the axial methionine ligand is replaced by another amino acid residue (e.g., glutamine in stellacyanin and umecyanin).

These four groups have further been collected into two classes, based on their EPR characteristics. The first two groups display axial EPR signals that are characterized by an unusually small $A_{//}$ hyperfine coupling constant (as compared to normal inorganic Cu(II) centers). On the other hand, stellacyanin (group 4) and the proteins of the third group show rhombic EPR spectra, with a varying degree of rhombic distortion. Furthermore, as pointed out by Lu et al.,[4] a correlation exists between the EPR characteristics of blue copper proteins and their electronic spectra. The absorption spectra of axial type 1 proteins are characterized by one dominating feature around 600 nm (the blue band), while in the spectra of rhombic type 1 proteins an additional feature appears around 460 nm, at the expense of the 600 nm band. The intensity ratio $\epsilon_{460}/\epsilon_{600}$ is 0.06 in plastocyanin and 0.11 in azurin, indicating that the 460 nm band is also present in the axial type 1 proteins, but very weak. In the rhombic proteins, on the other hand, $\epsilon_{460}/\epsilon_{600}$ ratios of 0.29, 0.41, 0.60, and 1.22 are found for stellacyanin, pseudoazurin, cucumber basic protein and, nitrite reductase, respectively. Interestingly, this series is also conform with the extent of rhombic distortion found in the EPR spectra, with nitrite reductase presenting a limiting case of a strongly perturbed site in both cases. This is an obvious indication that the rhombicity of the EPR spectra and the intensity of the 460 nm band have a common structural basis.

In a previous study,[5] we have examined the relationship between the structure and spectroscopic properties of the series plastocyanin, pseudoazurin, cucumber basic protein, and nitrite reductase, four proteins with the same four copper ligands. The distinction between axial and rhombic type 1 proteins was connected to a different ground-state electronic structure in both classes of proteins, connected in turn to a different geometry. Plastocyanin and the other axial type 1 proteins are characterized by a trigonal structure, gaining its stability from a strongly covalent $Cu-S_{Cys}$ π interaction, combined with a σ interaction

S1089-5647(98)00455-6 CCC: $15.00
Published on Web 05/14/1998

with the two N_{His} ligands. The fourth, axial S_{Met} ligand is found at a large distance, and its interaction with copper is purely electrostatic. On the other hand, the structure of rhombic type 1 proteins is considerably flattened with respect to a trigonal structure. A convenient way to quantify this flattening is by considering the angle between the planes formed by $N_{His}-Cu-N_{His}$ and $S_{Cys}-Cu-S_{Met}$, denoted as ϕ. In a strictly trigonal structure, both planes are perpendicular ($\phi = 90°$). In practice, axial type 1 proteins have ϕ angles ranging between 77° and 89°. In the rhombic type 1 proteins, on the other hand, considerably smaller ϕ angles are found, ranging between 56° and 75°. In the limit of $\phi = 0°$, a strictly tetragonal structure is formed, with four strong σ bonds to the copper ion, instead of the three (two σ + one π) strong interactions found in a trigonal structure. Intermediate ϕ angles also give intermediate electronic interactions, and in the rhombic type 1 proteins, the $Cu-S_{Cys}$ interaction indeed contains both π and σ components, while a σ bond between Cu and S_{Met} is formed. This is also apparent from the crystal structures of these proteins, indicating a considerably shorter $Cu-S_{Met}$ bond and a longer $Cu-S_{Cys}$ bond in the rhombic type 1 proteins as compared to plastocyanin.[6]

The different electronic ground-state structure between the axial and rhombic type 1 proteins also nicely explains the differences found in their electronic spectra. It was shown that the bands at 460 and 600 nm correspond to an excitation originating from the $Cu-S_{Cys}$ σ and π bonding orbitals, respectively. As such, the relative intensity of both bands depends on the character of the orbital which is singly occupied in the ground state. In the axial proteins, this orbital is purely π antibonding between Cu and S_{Cys}, and the 460 nm band therefore has little or no intensity. In the rhombic proteins on the other hand, the ground-state singly occupied orbital gains more $Cu-S_{Cys}$ σ antibonding character as the structure becomes more flattened (smaller ϕ angle), resulting in an increased intensity of the 460 nm and a decreased intensity of the 600 nm band.

In this paper we describe the structural and spectral characteristics of stellacyanin and discuss differences and similarities to the other blue copper proteins. The main difference between stellacyanin and the proteins described above is, of course, the appearance of a new fourth ligand, replacing methionine. So far, the typical stellacyanin from *Rhus vernicifera* has resisted all crystallization attempts, probably because of the high carbohydrate content and heterogeneity caused by polyploidy or posttranslational modifications.[7,8] However, two crystal structures of proteins have been published that most likely resemble stellacyanin. In the Met121Gln azurin mutant,[9] the axial methionine ligand is replaced by a glutamine residue. This substitution leads to spectral properties that are almost identical to those of stellacyanin. Recently, the crystal structure of a stellacyanin from cucumber was produced.[10] In fact, it is a recombinant stellacyanin that has been crystallized after removal of the non-copper binding domains and glycosylation sites by site-directed mutagenesis.[11] In this way, the glycosylation and heterogenity present in *Rhus vernicifera* stellacyanin was avoided. Our calculations are based on the former structure, because its spectral properties are almost equal to those of stellacyanin and this was the only structure available at the time when the investigation was initiated.

Apart from the presence of a different axial ligand, the copper coordination geometry in the crystal structure of the Met121Gln azurin mutant is close to the one of plastocyanin. In particular, the angle ϕ between the O−Cu−S and N−Cu−N planes is 82−86°, within the range found for the type 1 proteins with a trigonal structure. Yet, the spectral characteristics of stellacyanin clearly point to a rhombic type 1 protein. As such, stellacyanin forms an exception to the relation between the structure and the spectral properties found for the more normal blue copper proteins with a methionine ligand. In this work, we will investigate the origin of this exceptional behavior, and in particular, the role played by the axial glutamine amino acid.

Furthermore, we have also studied the structure and spectrum of some stellacyanin models with alternative axial ligands. The spectrum of stellacyanin is pH dependent: at high pH, the blue band shifts from 610 to 580 nm.[7] It has been suggested that this blue shift is due to a change in the copper ligand sphere. At high pH, the N^{ϵ} atom of the glutamine ligand may loose one proton and replace the O^{ϵ} atom as a copper ligand.[7,12] However, this hypothesis has recently been challenged.[11] To resolve this controvercy, we have investigated if the calculated spectrum of models with N^{ϵ} coordinating to copper may reproduce the observed spectral shifts.

2. Methods

2.1. Geometry Optimizations. The geometry of the active site of stellacyanin has been modeled with the same methods we have used for other blue copper proteins.[5,13−15] The histidine ligands are modeled by ammonia or imidazole, the cysteine residue by SH^- or SCH_3^-, and the glutamine residue by formaldehyde (H_2CO), formamide ($HCONH_2$), or acetamide (CH_3CONH_2).

Structures of different model complexes were optimized using the hybrid density functional method B3LYP as implemented in the MULLIKEN-2.31h[16] or in GAUSSIAN-94[17] software. Hybrid density functional methods have been shown to give as good or better geometries as correlated ab initio methods for first-row transition metal complexes.[18] The 6-31G* basis sets were used for all atoms, except for the copper atom, for which we used the double-ζ copper basis (62111111/33111/311) of Schäfer et al,[19] enhanced with diffuse p, d, and f functions with exponents 0.174, 0.132, and 0.39. The coordinate system was defined as before:[13] the copper ion is placed at the origin, the $Cu-O_{Gln}$ bond is along the *z* axis, and the $Cu-S_{Cys}$ bond is situated in the *xz* plane.

2.2. Spectral Calculations. Calculations of the electronic spectra were performed using the CASSCF−CASPT2 approach (second-order perturbation theory with a multiconfigurational reference state).[20] Most of the calculations were performed without symmetry. The CASSCF active space then consisted of 13 electrons distributed in 12 orbitals, chosen as follows: five Cu3d orbitals, five correlating Cu3d′ orbitals, and the S_{Cys}-$3p_{\sigma}$ and p_{π} lone-pair orbitals. With this active space, it is possible to describe the ground state and the six lowest excited states in the spectrum. Some test calculations were also performed on models with C_s symmetry. In this case, the active space could be limited to 11 orbitals, since the $S_{Cys}3p_{\sigma}$ and S_{Cys}-$3p_{\pi}$ orbitals belong to different representations. In all cases, one state-average CASSCF calculation over all states belonging to a given symmetry was performed, followed by a CASPT2 calculation on each state. In the CASPT2 calculations all electrons originating from the S3s,3p, C2s,2p, N2s,2p, O2s,2p, H1s, and Cu3s,3p were correlated.

The basis sets used in the CASSCF/CASPT2 calculations were of the generally contracted atomic natural orbital (ANO) type,[21] contracted in the following way: Cu [17s12p9d1f/6s4p3d1f], S [13s10p4d/4s3p1d], O [10s6p3d/3s2p1d], N [10s6p/3s2p], C [10s6p/3s2p], H [7s/2s] for the hydrogens bound to

S_{Cys}, and [7s/1s] for the hydrogens bound to N or C when histidine was modeled by imidazole. For the ammonia model, all hydrogens had the [7s/2s] contraction. Previous work has shown that these moderate-size contractions are sufficient to give a proper description of the spectra of blue copper proteins.[5,13,14]

Relativistic corrections (Darwin and mass-velocity), obtained at the CASSCF level, were added to the CASPT2 excitation energies. A level shift, added to the zeroth-order Hamiltonian, was used to remove intruder states. This technique has been investigated thoroughly on the $Cu(imidazole)_2(SH)(SH_2)^+$ system, where it was shown that a level shift of 0.3 is appropriate to remove all intruder states without deteriorating the excitation energies.[20] This value was also used successfully for the present systems. Oscillator strengths were obtained from the transition dipole moments computed with the CAS state-interaction method[22] at the CASSCF level in combination with CASPT2 excitation energies. The CASSCF/CASPT2 calculations were performed with the MOLCAS-3.1 quantum chemistry software,[23] and all calculations were run on IBM RS/6000 workstations.

2.3. A Model of the Surrounding Protein and Solvent. A calculation of the spectrum was also performed on $Cu(imidazole)_2(SH)[OCH(NH_2)]^+$ without symmetry, using the experimental geometry of the copper ion in the A subunit of the Met121Gln azurin mutant[9] (PDB file 1URI). The system was truncated by hydrogen atoms placed at standard bond lengths in the direction of the removed carbon atom.

To estimate the effect of the surrounding protein, a second set of calculations was performed on this model, surrounded by 5851 point charges, representing the remaining protein atoms in the two subunits of the protein (except those atoms connected to the atoms that were converted to hydrogen atoms in the model system), all crystal−water molecules, and a sphere of solvent water molecules with a radius of 2.4 nm. All Asp and Glu residues were treated as anions and all Lys and Arg residues as cations. The protonation status of the histidine residues were decided from the hydrogen-bond pattern: His-32 was found to have protons on both nitrogens, His-83 was protonated on the $N^{\delta 1}$ atom, whereas His-35, -42, and -117 were protonated on the $N^{\epsilon 2}$ atom. Each atom was assigned a point charge, taken from the Amber 4.1 force field.[24]

The positions of the solvent water molecules and the protein hydrogen atoms were determined by a 22.5 ps simulated annealing molecular dynamics simulation. The temperature was kept at 300 K during the first 7.5 ps and was then decreased linearly with time to 0 K at the end of the simulation. The charges on the copper ion and its ligands were taken from a quantum mechanical calculation on $Cu(imidazole)_2(SH)(OCH(NH_2)^+$ without symmetry. The software Amber version 4.1[25] was used. Further computational details can be found for the analogous equilibration of plastocyanin.[14]

3. Geometric Features

In Table 1 we have collected the structures obtained from the B3LYP optimizations on some relevant model compounds. Calculations without symmetry were performed for the models $Cu(NH_3)_2(SH)[OCH(NH_2)]^+$, $Cu(NH_3)_2(SCH_3)[OCH(NH_2)]^+$, and $Cu(NH_3)_2(SH)[OC(CH_3)(NH_2)]^+$. Figure 1 shows the result for $Cu(NH_3)_2(SH)[OCH(NH_2)]^+$. In accord with our earlier investigations,[15] two different structures were obtained for all three complexes: a trigonal and a tetragonal. Both structures are stable local minima, judging from vibrational frequency analyses performed on the $Cu(NH_3)_2(SH)[OCH(NH_2)]^+$ models

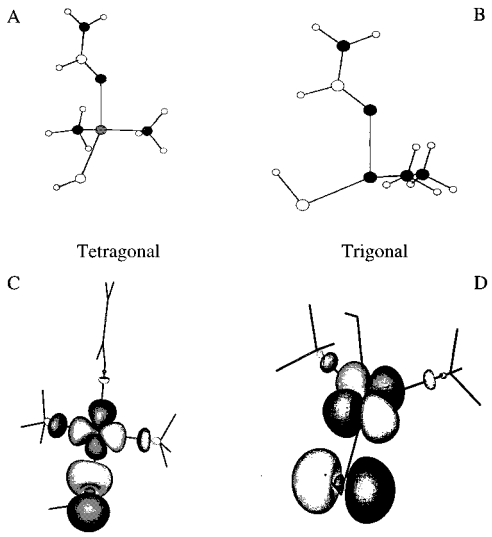

Figure 1. The optimized (A) tetragonal and (B) trigonal structures of the $Cu(NH_3)(SH)[OCH(NH_2)]^+$ model. C and D show the corresponding singly occupied natural orbital of the ground state of structure A and B.

(results not shown). They are characterized by different metal−ligand bond distances and angles. In the tetragonal structures, four σ bonds are formed between the central copper ion and the ligands. As such, we find here a considerably (about 0.2 Å) shorter Cu−O distance than in the trigonal structures, where only three strong copper−ligand bonds are formed, and the Gln oxygen becomes a weakly bonded axial ligand. This can also be seen from Figure 1C and D, showing the orbital that is singly occupied in the ground states of both structures. In the tetragonal structure, the four lobes of the Cu3d orbital overlap with a p_σ orbital from each of the four ligands, while in the trigonal structure two σ bonds have been replaced by a π bond with the sulfur $3p_\pi$ orbital. This π bond gives rise to a shorter Cu−S distance, as indicated by the fact that systematically shorter Cu−S bonds are found (about 0.07 Å) in the trigonal structures as compared to the tetragonal structures.

The present results are similar to what was found in our previous studies[5,15] on the blue copper proteins with methionine instead of glutamine as the fourth ligand. In fact, except for the shorter Cu−O as compared to the Cu−S distance, both structures obtained in this work for $Cu(NH_3)_2(SH)[OCH(NH_2)]^+$ (Figure 1) are very close to the two minima found for the simple $Cu(NH_3)_2(SH)(SH_2)^+$ model used in these studies, with distances differing by less than 0.02 Å and angles by less than 10°. Notably, for $Cu(NH_3)_2(SH)(SH_2)^+$, and also for all models studied in this work, the tetragonal minimum is found to have its two NH_3 ligands positioned trans with respect to each other. This is not the conformation found in the crystal structure of for example nitrite reductase, a typical tetragonally distorted protein, or in the tetragonal minima found for some of the larger model compounds such as $Cu(NH_3)_2(SH)S(CH_3)_2^+$,[5] where the N−Cu−N angle remains close to 90°, indicating a cis conformation, and each of the NH_3 is instead found opposite to one of the S ligands. The important point is, however, that both conformations, and also the trigonal structure, have very similar energies, indicating that the potential surface for rotation of the various ligands around the central Cu is extremely flat.[15] This is also the case for the models considered in this work. As one can see from Table 1, the energy difference between the trigonal and tetragonal structures is at most 7.0 kJ/mol, with the trigonal structure being most stable for $Cu(NH_3)_2(SCH_3)[OCH(NH_2)]^+$, and the tetragonal structure most stable for the other two models

TABLE 1: Distances and Angles around the Copper Ion in the B3LYP-optimized Structures[a]

			distances to Cu				angle subtented at Cu						dihedral		
		ΔE (kJ/mole)	Ax_{Gln}	S_{Cys}	N_{His1}	N_{His2}	Ax−S	Ax−N_1	Ax−N_2	S−N_1	S−N_2	N−N	X_{Cys}−Ax	S−C_{Gln}	ϕ
$Cu(NH_3)_2(SH)[OCH(NH_2)]^+$															
C_1 *tetra*	^{2}A	0.0	2.09	2.25	2.05	2.04	153	92	90	92	99	152	101	3	
C_1 *trig*	^{2}A	1.6	2.27	2.17	2.06	2.06	116	88	87	126	125	103	0	6	89
C_s *trans*	^{2}A″	1.6	2.27	2.17	2.06	2.06	116	87	87	125	125	103	0	0	90
C_s *cis*	^{2}A″	7.0	2.36	2.16	2.05	2.05	120	83	83	126	126	102	0	0	90
$Cu(NH_3)_2(SCH_3)[OCH(NH_2)]^+$															
C_1 *tetra*	^{2}A	3.0	2.10	2.23	2.07	2.06	141	94	93	94	105	138	102	3	
C_1 *trig*	^{2}A	0.0	2.35	2.16	2.08	2.06	118	88	82	125	126	104	1	30	86
C_s *trans*	^{2}A″	0.2	2.34	2.16	2.07	2.07	120	85	85	125	125	103	0	0	90
$Cu(NH_3)_2(SH)[OC(CH_3)(NH_2)]^+$															
C_1 *tetra*	^{2}A	0.0	2.06	2.24	2.06	2.06	153	92	91	92	99	149	102	4	
C_1 *trig*	^{2}A	7.0	2.27	2.17	2.05	2.07	116	84	91	124	127	103	2	33	85
C_s *trans*	^{2}A″	7.0	2.29	2.17	2.06	2.06	121	85	85	125	125	103	0	0	90
$Cu(imidazole)_2(SH)[OCH(NH_2)]^+$															
C_1 *trig*	^{2}A	0.0	2.28	2.18	2.01	2.02	108	90	101	133	117	101	−2	−42	82
C_s *trans*	^{2}A″	2.7	2.35	2.17	2.02	2.02	112	91	91	125	125	102	0	0	90
$Cu(imidazole)_2(SH)[OC(CH_3)(NH_2)]^+$															
C_1 *tetra*	^{2}A		2.12	2.26	1.99	2.01	138	94	94	100	97	144	83	14	
$Cu(imidazole)_2(SCH_3)[OC(CH_3)(NH_2)]^+$															
C_1 *tetra*	^{2}A	0.0	2.12	2.25	1.99	2.04	138	94	94	104	98	137	75	16	
C_1 *trig*	^{2}A	2.2	2.24	2.17	2.02	2.06	113	92	95	125	122	103	−15	−54	88
$Cu(NH_3)_2(SH)[(NH)H(CO)]$															
C_1 *tetra*	^{2}A	0.0	1.98	2.28	2.09	2.08	175	90	89	87	95	175	135	137	
C_s *trans*	^{2}A″	51.0	2.08	2.19	2.12	2.12	113	97	97	119	119	107	0	0	90
crystal structures															
Met121Glu Azurin Subunit A[9]			2.25	2.13	1.91	2.06	107	87	98	141	116	97	1	−80	82
Met121Glu Azurin Subunit B[9]			2.27	2.11	1.96	2.03	103	91	97	133	117	105	−1	−71	86
cucumber stellacyanin[10]			2.21	2.18	1.96	2.04	101	94	102	134	118	101	−1	−71	83

[a] Distances in angstroms, angles in degrees. Ax = O_{Gln}, except for the two $Cu(NH_3)_2(SH)[(NH)H(CO)]$ structure where Ax = N_{Gln}.

($Cu(NH_3)_2(SH)[OCH(NH_2)]^+$ and $Cu(NH_3)_2(SH)[OC(CH_3)(NH_2)]^+$). Such a flat potential surface also means that either structure, as well as any intermediate structure, may be stabilized by the protein environment. In the crystal structure of the Met121Gln azurin mutant, the copper surrounding is obviously close to trigonal. This is indicated by the short Cu−S and the long Cu−O bond, both corresponding well to the calculated distances in the trigonal models, and by the angles between the various ligands, shown in Table 1.

For the trigonal structures, we have included in the last column of Table 1 the value of ϕ (i.e., the angle between the planes formed by the N−Cu−N and S−Cu−O bonds). The value of ϕ gives an indication of how close the structures are to "ideal" trigonal. Indeed, in a strictly trigonal structure, ϕ = 90°, and the S−Cu−O plane becomes a symmetry plane, mirroring the two N-bonded ligands. As one can see from the ϕ angles in Table 1, the trigonal model structures, optimized without symmetry, are very close to, but not strictly trigonal. When analyzing the different bond distances and angles, it is clear that the most important deviation from C_s symmetry comes from the orientation of the Gln ligand. In a C_s structure, the Gln residue must lie in the symmetry plane of the molecule, while in the actual C_1 structures, a rotation out of this plane by 3−33° is found. To estimate the energetic consequence of this rotation, a second set of optimizations was performed on the trigonal structures, now using C_s symmetry, with the Gln residue forced to lie in the symmetry plane of the molecule. Two different orientations in this plane are possible, with the amine group situated either cis or trans to copper with respect to the O═C bond. The most important geometrical features of both the cis and trans structures of $Cu(NH_3)_2(SH)[OCH(NH_2)]^+$ are shown in Table 1. For this small model, the trans structure is closer to the crystal structure than the cis structure: the latter has a 0.1 Å too long Cu−O bond. Moreover, the trans structure is 5.4 kJ/mol more stable than the cis structure. It is also clear from the structures in Table 1 that, apart from the different orientation of the Gln residues, the C_1 trigonal and the C_s trans structures are virtually indistinguishable. However, with more realistic models, the cis structure becomes also very close to the crystal structure, which is in fact in the cis conformation.

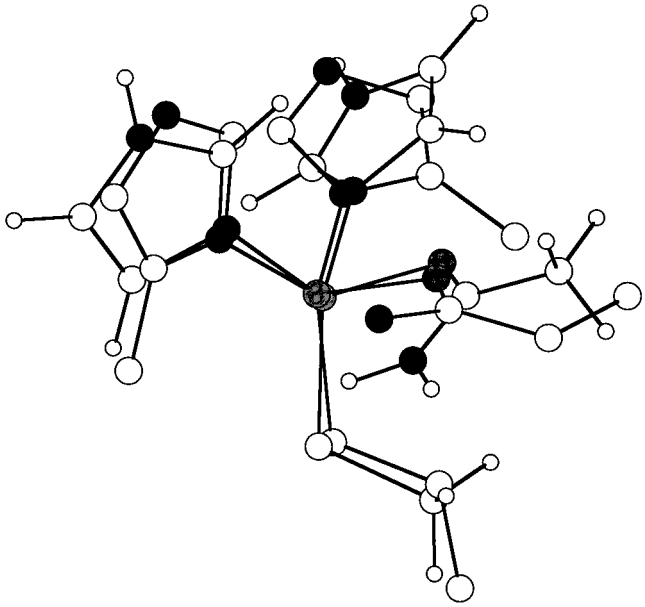

Figure 2. Comparison of the optimized trigonal C_1 structure of Cu(imidazole)$_2$(SH)[OC(CH$_3$)(NH$_2$)]$^+$ and the crystal structure of cucumber stellacyanin[10] (no hydrogen atoms).

Our best optimized model of stellacyanin is the trigonal C_1 structure of $Cu(imidazole)_2(SCH_3)[OC(CH_3)(NH_2)]^+$. In Figure 2, this structure is compared to the crystal structure of cucumber stellacyanin,[10] and in Table 1, the geometry around the copper ion of the optimized structure is compared with all available crystal structures.[9,10] It can be seen from the table that the

TABLE 2: Comparison of the Spectra Calculated for Plastocyanin and Stellacyanin

	excitation energy(oscillator strength)					
final state C_s	A[a]	B	C	D	E	final state C_1
			plastocyanin[14]			
a ^{2}A′	3 880	5 411	4 836	3 901	5 000	b ^{2}A
b ^{2}A′	11 577	14 475	12 537	10 854	10 800(0.0031)	c ^{2}A
b ^{2}A″	12 996(0.0014)	15 356(0.0028)	13 556(0.0015)	13 023	12 800(0.0114)	d ^{2}A
c ^{2}A′	12 821	15 084(0.0004)	13 235(0.0003)	13 489	13 950(0.0043)	e ^{2}A
c ^{2}A″	12 393(0.0886)	15 948(0.1189)	16 970(0.1032)	17 500	16 700(0.0496)	f ^{2}A
d ^{2}A′	20 243(0.0008)	22 093(0.0010)	23 156(0.0014)	20 511	21 390(0.0035)	g ^{2}A
			stellacyanin			
a ^{2}A′	3 507	4 897(0.0002)	4 947	5 203		b ^{2}A
b ^{2}A′	9 491	11 740	10 003	12 278		c ^{2}A
b ^{2}A″	12 121(0.0011)	13 729(0.0010)	12 056(0.0006)	14 207	11 800(0.0075)	d ^{2}A
c ^{2}A′	12 133	13 265	11 548	13 846		e ^{2}A
c ^{2}A″	13 158(0.0818)	13 928(0.0821)	16 705(0.0748)	17 052	16 600(0.0330)	f ^{2}A
d ^{2}A′	20 987(0.0009)	20 890(0.0153)	23 510(0.0118)	22 235	22 300(0.0040)	g ^{2}A

[a] (A) Optimized geometry using C_s symmetry; (B) experimental geometry; (C) experimental geometry with surrounding point pointcharges; (D) same as C but corrected for the effects of replacing SH by SCH_3, SH_2 by $S(CH_3)_2$, and $OCH(NH_2)$ by $OC(CH_3)(NH_2)$ (corrections taken from Table 4 and from Table 7 in ref 14; (E) experimental excitation energies and oscillator strengths.[7,30]

optimized structure is very similar to the crystal structures. The optimized $Cu-S_{Cys}$ and $Cu-O_{Gln}$ bond lengths differ by less than 0.03 Å from the average crystal values. The two optimized Cu−N distances (2.02−2.06 Å) are inside the range encountered in the crystals and rather close to the average (1.99 Å), but the variation is less than in the crystals. The average difference between the optimized angles around the copper ion and the average values in the crystals is 5°, and the largest deviation is 11° (for one of the S−Cu−N angles). The only significant differences between the optimized structure and the crystal structures is the orientation of the glutamine residue and one of the histidine rings. The imidazole ring has rotated about 60° compared to the crystal structure, whereas the glutamine model has rotated 30°. However, these dihedral motions have little influence on the energy of the complex and they are most likely dictated by the folding of the amino acid backbone the protein. The close similarity between the optimized structure in a vacuum and the crystal structures, clearly show that the oxidized structure of the blue copper proteins is not strained by the protein, as the induced-rack and entatic state theories suggest.[26,27] This is in accord with our ealier investigations on plastocyanin.[13]

Interestingly, the average ϕ angles in the crystal structures is 84°, which is sligthly less than the value found in our best optimized structure (88°) but somewhat larger than the value in the crystal structure of plastocyanin, the typical example of a trigonal blue copper protein (82°). Thus, it is clear, that as far as the structure is concerned, stellacyanin can be classified among the trigonal blue copper proteins.

4. Comparison of the Electronic Structure and Spectrum of Stellacyanin and Plastocyanin

Despite the fact that plastocyanin and stellacyanin have a similar copper coordination geometry in the crystal structure, the electronic spectra of the two enzymes show distinct differences: the characteristic blue band around 16600 cm^{-1} (600 nm), dominant in plastocyanin, becomes considerably weaker in stellacyanin, where, on the other hand, a band around 22000 cm^{-1} (460 nm) gains intensity. A detailed analysis of the electronic spectrum of plastocyanin has been presented previously.[14] It was shown there that the two bands under consideration are due to charge-transfer excitation from the cysteine $S3p_\pi$ and $S3p_\sigma$ orbitals into the Cu3d shell. Here, we present a comparison of the calculated electronic spectra of Cu(imidazole)$_2$(SH)[$OCH(NH_2)$]$^+$ and Cu(imidazole)$_2$(SH)$(SH_2)^+$ as a model for stellacyanin and plastocyanin, respectively. Spectra were calculated both for the B3LYP trigonal structures with C_s symmetry and for the crystal structures, with and without surrounding point charges. The results are shown in Table 2. In Table 3, we have collected the main atomic orbital components of the orbital that is singly occupied in the ground state and in the different calculated excited states. These orbitals are useful to characterize the electronic structure of the different states. Figure 3 shows the orbitals obtained for Cu(imidazole)$_2$-(SH)[$OCH(NH_2)$]$^+$, at the Met121Gln azurin crystal structure.

As was already shown for Cu$(NH_3)_2$(SH)[$OCH(NH_2)$]$^+$ (Figure 1), the electronic ground state connected with a trigonal structure is characterized by a π (anti-) bond between copper and the cysteine sulfur. This is further illustrated by the composition of the X ^{2}A″ ground-state singly occupied orbital in the two C_s models. In both cases, this orbital consists of an antibonding combination of $Cu3d_{xy}$ (80−82°), and S_{Cys} $3p_\pi$ (15−18%). All other contributions are small, including the one from the imidazole nitrogen ligands (slightly less than 1%). The corresponding bonding combination, with predominantly S_{Cys}-$3p_\pi$ character, is the singly occupied orbital in the c ^{2}A excited state. As such, the X ^{2}A″ → c ^{2}A″ transition corresponds to a S_{Cys}-to-Cu charge-transfer excitation, gaining intensity from the strong overlap between both orbitals involved. Indeed, as indicated by the results in column A of Table 2, the X ^{2}A″ → c ^{2}A″ transition is by far the most intense transition in the electronic spectra of both C_s model compounds. Even if, in the optimized C_s structures, the calculated excitation energy is 3000−4000 cm^{-1} too low as compared to experiment, this transition obviously corresponds to the dominant "blue" band around 16600 cm^{-1} in the electronic spectra of both proteins.

The singly occupied orbitals corresponding to the excited states a ^{2}A′ and d ^{2}A′ both show a delocalization over the Cu−S_{Cys} σ bond. The orbital corresponding to the a ^{2}A′ state is antibonding and has predominantly (63%) $Cu3d_{x^2-y^2}$ character, while the corresponding bonding orbital, mainly $S_{Cys}3p_\sigma$, is depopulated in the d ^{2}A′ excited state. The X ^{2}A″ → d ^{2}A′ transition thus also involves a S_{Cys} → Cu charge-transfer. However, due to the fact that, in the C_s models, both orbitals involved belong to different symmetries, there is no overlap and the intensity of the transition is low. This is true both for the plastocyanin and stellacyanin models.

TABLE 3: Composition (%) of the Singly Occupied Orbital in the Ground State and the Different Excited States of the Cu(imidazole)$_2$(SH)(SH$_2$)$^+$ (Plastocyanin) and Cu(imidazole)$_2$(SH)[OCH(NH$_2$)]$^+$ (Stellacyanin) Models, at the C_s-Optimized Geometries and the Experimental Crystal Structures

A. C_s-Optimized Models

			STATE						
protein	atomic orbital		X ^{2}A″	a ^{2}A′	b ^{2}A′	b ^{2}A″	c ^{2}A′	c ^{2}A″	d ^{2}A′
stellacyanin	Cu	3d_{xy}	82	0	0	3	0	14	0
		3d_{yz}	2	0	0	95	0	3	0
		3$d_{x^2-y^2}$	0	63	3	0	18	0	15
		3d_{z^2}	0	1	95	0	0	0	2
		3d_{xz}	0	14	0	0	81	0	5
		4*s*,4*p*	0	6	1	0	0	1	10
	S_{Cys}	3p_σ	0	16	0	0	0	0	67
	S_{Cys}	3p_π	15	0	0	1	0	82	0
plastocyanin	Cu	3d_{xy}	80	0	0	2	0	17	0
		3d_{yz}	1	0	0	96	0	3	0
		3$d_{x^2-y^2}$	0	63	7	0	10	0	19
		3d_{z^2}	0	2	89	0	5	0	3
		3d_{xz}	0	9	2	0	84	0	4
		4*s*,4*p*	0	7	1	0	0	1	10
	S_{Cys}	3p_σ	0	19	0	0	0	0	63
	S_{Cys}	3p_π	18	0	0	1	0	78	0

B. Experimental Crystal Structures.

			STATE						
protein	atomic orbital		X ^{2}A	b ^{2}A	c ^{2}A	d ^{2}A	e ^{2}A	f ^{2}A	g ^{2}A
stellacyanin	Cu	3d_{xy}	59	26	0	0	0	11	1
		3d_{yz}	0	3	2	82	13	1	0
		3$d_{x^2-y^2}$	18	40	13	8	7	1	13
		3d_{z^2}	3	9	83	1	0	0	3
		3d_{xz}	3	0	1	8	80	0	2
		4*s*,4*p*	2	4	0	0	0	1	9
	S_{Cys}	3p_σ	3	11	0	0	0	2	69
	S_{Cys}	3p_π	9	3	0	1	0	83	2
plastocyanin	Cu	3d_{xy}	78	2	0	1	1	16	0
		3d_{yz}	0	1	9	77	11	3	0
		3$d_{x^2-y^2}$	1	57	16	6	2	0	17
		3d_{z^2}	0	8	68	1	17	0	5
		3d_{xz}	1	8	5	14	68	0	3
		4*s*,4*p*	0	6	0	0	0	1	7
	S_{Cys}	3p_σ	0	18	0	0	0	0	66
	S_{Cys}	3p_π	17	0	0	1	0	78	0

Below the charge-transfer states, three ligand-field states, b ^{2}A′, b ^{2}A″, and c ^{2}A″, are calculated, corresponding to an excitation from the Cu3d$_{z^2}$, -3d$_{yz}$ and -3d$_{xz}$ orbitals, respectively. Only the transition to b ^{2}A″ is predicted to have some intensity, due to the mixing in of a small amount of $S_{Cys}3p_\pi$ character in the corresponding 3d$_{yz}$ singly occupied orbital (with the same symmetry). The transitions to c ^{2}A′ and c ^{2}A″ are calculated at about the same energy in the plastocyanin and stellacyanin models. However, the b ^{2}A′ state is found at a considerably lower energy in stellacyanin. This is a reflection of the different axial field in the latter protein. Indeed, the corresponding transition originates from the Cu3d$_{z^2}$ orbital, pointing toward a different axial ligand in the two proteins.

Apart from the difference in excitation energy of the b ^{2}A′ state, the electronic spectra of the C_s plastocyanin and stellacyanin models are similar, both as concerns excitation energies and oscillator strengths. In particular, the shifts in intensities observed in the experimental spectrum of stellacyanin as compared to plastocyanin, are not reproduced by these models.

However, when looking at the spectra obtained for the crystal structures (columns B and C in Table 2), the correct shifts appear. No symmetry is left in these structures, such that states belonging to different symmetries within C_s are now allowed to mix. In practice, little mixing is observed in the plastocyanin model. This can be seen from the composition of the singly occupied orbitals in Table 3, showing only small variations in the C_1 as compared to the C_s plastocyanin model. In the case of stellacyanin, however, much larger variations are found. This is especially true for the singly occupied orbitals corresponding to the ground-state X ^{2}A and the first excited-state b ^{2}A, where a strong mixing between 3d$_{xy}$ (π bonding with S_{Cys}) and 3d$_{x^2-y^2}$ (σ bonding with S_{Cys}) is observed for the C_1 structure. The mixing is also nicely illustrated by the orbital plots in Figure 3. In the corresponding bonding orbitals, singly occupied in the two highest states f,g ^{2}A, the corresponding mixing is much less pronounced. As a consequence, the two $S_{Cys} \rightarrow$ Cu3d charge-transfer excitations in the spectrum of stellacyanin still originate from a S_{Cys}3p orbital which is either pure π or σ, yet the electron is excited into an orbital with mixed π, σ character. This explains the partial shift in intensity from the blue band (16700 cm^{-1}) to the higher-lying charge-transfer band at 22300 cm^{-1} in the stellacyanin as compared to the plastocyanin spectrum. This shift is, at least qualitatively, reproduced by the calculated results in Table 2 (columns B and C).

Similar observations were also made in our study of the electronic spectra of the series of blue copper proteins plastocyanin, pseudoazurin, cucumber basic protein, and nitrite reductase.[5] There, we found that the increasing intensity of the second charge-transfer band within the series is connected to an increasing tetragonal structural distortion of the copper ligand surrounding, exemplified by the angle ϕ between the N−Cu−N and the S−Cu−S planes. However, the crystal structures of

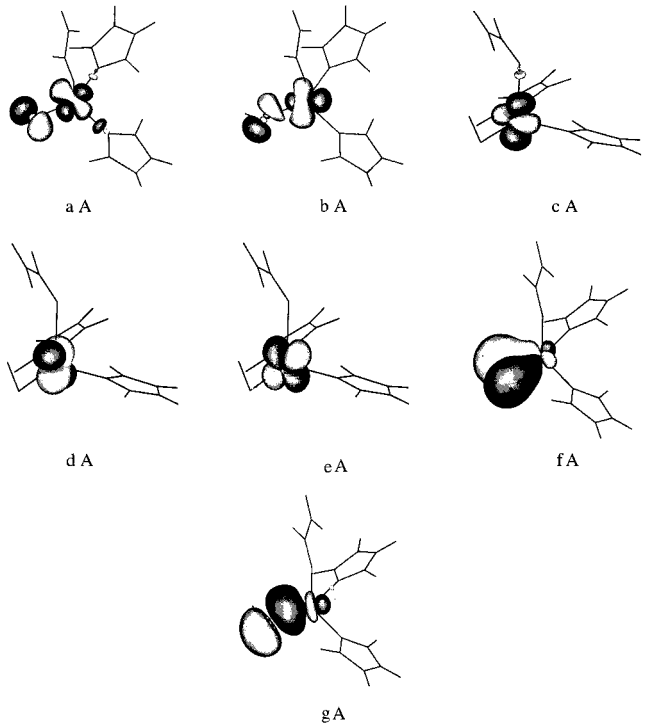

Figure 3. The singly occupied natural orbitals for the ground state and the six lowest excited states of Cu(imidazole)$_2$(SH)[OCH(NH$_2$)]$^+$ at the crystal structure geometry.

both stellacyanin and plastocyanin are characterized by the same ϕ angle (82°). The explanation for the shift in intensity in the stellacyanin spectrum can thus not be brought back to structural differences, but must instead be connected to the different axial ligand, glutamine instead of methionine. The role played by the axial glutamine ligand will be examined in more detail in the next section.

As concerns the calculated excitation energies, we find some notable differences between the results obtained for plastocyanin and stellacyanin. In our previous study of the plastocyanin spectrum[14] it was already shown that the calculated excitation energies strongly depend on the model structure, and in particular on the Cu−S$_{Cys}$ distance. This is reflected by the differences in excitation energies between the C_s model and the experimental structure of Cu(imidazole)$_2$(SH)(SH$_2$)$^+$ (columns A and B in Table 2). In the experimental plastocyanin structure, the Cu−S$_{Cys}$ distance is 2.07 Å,[28] while in the C_s model, a distance of 2.17 Å is found.[14] The difference, 0.1 Å, is responsible for large shifts in the calculated excitation energies, up to 3500 cm^{-1} (for the blue band). For Cu(imidazole)$_2$(SH)-[OCH(NH$_2$)]$^+$ the difference in Cu−S$_{Cys}$ distance between the C_s model and the crystal structure, 0.04 Å, is smaller, as are the differences in the calculated excitation energies. The latter is especially true for the two charge-transfer states, with shifts of only 770 and −97 cm^{-1} respectively. As a consequence, the excitation energies obtained for the crystal model of stellacyanin are considerably lower than for plastocyanin, and also lower than the experimental results. However, the situation is restored after adding the effect of the crystal environment (column C in Table 2). Indeed, the effect on the excitation energies of adding surrounding point charges to the crystal models is, at least for the two charge-transfer excitations, considerably larger for Cu(imidazole)$_2$(SH)[OCH(NH$_2$)]$^+$ than for Cu(imidazole)$_2$(SH)(SH$_2$)$^+$: 2700 cm^{-1} versus 1000 cm^{-1}. The effect of the crystal surrounding on the excitation energies can be connected to the change in polarity of the Cu−S$_{Cys}$ bond during the transitions. The effect is negative and of comparable magnitude (−1700 to −2000 cm^{-1}) in stellacyanin and plastocyanin for the ligand-field transitions, involving a charge flow from Cu to S$_{Cys}$, while it is positive and more pronounced for stellacyanin than for plastocyanin for the charge-transfer states, with a charge flow in the opposite direction. The first excited state does not change the polarity of the Cu−S$_{Cys}$ bond, and here the effect of the surrounding crystal is small for both proteins.

Finally, we have also examined the effect on the electronic excitations of going to larger model ligands for cysteine, methionine and glutamine, by replacing H by CH$_3$. The results are shown in column D of Table 2. For plastocyanin, they were taken from ref 14. For stellacyanin, they were obtained from a series of calculations on the C_s trans structures (shown in Table 1) of the models with NH$_3$ instead of imidazole. The results of these calculations are shown in Table 4. When OCH(NH$_2$) is replaced by OC(CH$_3$)NH$_2$ (column B), the transition energies hardly change. This is not surprising since the methyl group has to influence the copper through the double bond of the carbonyl group. On the other hand, when SH$^-$ is replaced by SCH$_3^-$ (column C), a larger effect is found: the ligand-field transitions increase by about 2300 cm^{-1}, the blue band increases by about 320 cm^{-1}, while the second charge-transfer band decreases by 1100 cm^{-1}. Column D shows the overall methyl substituting effect, which is taken into account in Table 2.

The final results obtained for the excitation energies, in column D of Table 2, compare well to the experimental values of the Met121Gln azurin mutant, shown in column E. For the two charge-transfer states, excellent agreement is obtained, with differences of less than 500 cm^{-1}. The band appearing at 11800 cm^{-1} in the experimental spectrum is assigned as the d ^{2}A state, corresponding to the ligand-field excitation out of the Cu3d$_{yz}$ orbital (see Table 3), and is calculated at 14207 cm^{-1}. This assignment is based on the fact that, even without symmetry, this is the only ligand-field transition that is found to have a significant oscillator strength. The error obtained for the excitation energy, 2400 cm^{-1}, is considerably higher than for the charge-transfer states, but is still considered to be acceptable.

5. Effect of the Axial Ligand in Blue Copper Proteins

An obvious way to study the effect of the fourth ligand on the spectroscopic properties of different blue copper proteins is to calculate the spectrum of an artificial model system, where this fourth ligand has been removed. Calculations along this line have been performed on Cu(imidazole)$_2$(SH)$^+$, using the crystal structure of plastocyanin and stellacyanin, respectively (without surrounding point charges). In addition, we have also added cucumber basic protein to the list (coordinates from the PDB file 2CBP). This protein has the same set of four ligands as plastocyanin, yet its spectrum is more akin to the stellacyanin spectrum, with two instead of one strong bands, and its sequence show a high homology (46%) with stellacyanin.[29]

A comparison of the calculated spectra of the different models, with and without the fourth ligand (SH$_2$ for plastocyanin and cucumber basic protein, OCH(NH$_2$) for stellacyanin) is presented in Table 5. Looking first at the excitation energies, we notice that the energies of the charge-transfer transitions hardly change when the axial ligand is removed (less than 360 cm^{-1}). This is not so surprising, since these transitions essentially take place within the Cu−S$_{Cys}$ bond. On the other hand, the ligand-field states are strongly affected. In all three cases, the removal of the axial ligand results in an increase of the ligand-field excitation energies. Again this is not surprising,

TABLE 4: Calculated Excitation Energies (cm^{-1}) and Oscillator Strengths (within Parentheses) of the C_s trans Structures of the Threee Different Stellacyanin Models, $Cu(NH_3)CysCln$

state	A Cys═SH^-, Gln═$OCH(NH_2)$	B Cys═SH^-, Gln═$OC(CH_3)(NH_2)$	C Cys═SCH_3^-, Gln═$OCH(NH_2)$	D global CH_3 effect
a $^2A'$	4 046(0.0000)	4 061(0.0000)	4 317(0.0000)	256
b $^2A'$	11 292(0.0000)	11 217(0.0000)	13 642(0.0000)	2 275
b $^2A''$	13 217(0.0019)	13 112(0.0020)	15 483(0.0046)	2 151
c $^2A'$	13 630(0.0000)	13 641(0.0000)	15 939(0.0000)	2 298
c $^2A''$	13 230(0.1126)	13 251(0.1122)	13 556(0.1341)	347
d $^2A'$	20 453(0.0004)	20 390(0.0006)	19 354(0.0005)	−1 275

TABLE 5: Influence of the Axial Ligand in Plastocyanin, Stellacyanin, and Cucumber Basic Protein at the Crystal Geometry. The excitation energies (cm^{-1}) and Oscillator Strengths (within Parentheses) Are Calculated with and without the Presence of the Axial Ligand

	plastocyanin		stellacyanin		cucumber basic protein	
state	with SH_2	no SH_2	with $OCH(NH_2)$	no $OCH(NH_2)$	with SH_2	no SH_2
b ^2A	5 411(0.0000)	6 513(0.0000)	4 897(0.0002)	5 874(0.0004)	4 861(0.0001)	5 409(0.0004)
c ^2A	14 475(0.0000)	15 840(0.0012)	11 740(0.0000)	15 089(0.0000)	12 878(0.0003)	15 056(0.0001)
d ^2A	15 356(0.0028)	16 632(0.0026)	13 729(0.0010)	15 729(0.0009)	14 699(0.0022)	15 811(0.0031)
e ^2A	15 084(0.0004)	16 152(0.0002)	13 265(0.0000)	15 340(0.0008)	14 586(0.0001)	14 944(0.0002)
f ^2A	15 948(0.1189)	16 111(0.1243)	13 928(0.0821)	13 570(0.0987)	13 535(0.0674)	13 533(0.0825)
g ^2A	22 093(0.0010)	22 381(0.0014)	20 890(0.0153)	20 710(0.0055)	20 505(0.0387)	20 526(0.0200)
R_{osc}^a	0.008	0.011	0.186	0.056	0.574	0.242

[a] R_{osc} is the ratio of the oscillator strengths of the g ^2A and f ^2A charge-transfer states.

TABLE 6: Influence of the Axial Ligand on the Composition (%) of the Ground-State Singly Occupied Orbital in $Cu(Im)_2(SH)(SH_2)^+$ (Plastocyanin and Cucumber Basic Protein) and $Cu(Im)_2(SH)[OCH(NH_2)]^+$ (Stellacyanin)

	atomic orbital contributions (%)								
	$Cu3d_{xy}$	$Cu3d_{yz}$	$Cu3d_{x^2-y^2}$	$Cu3d_{z^2}$	$Cu3d_{xz}$	Cu4*s*, 4*p*	$S_{Cys}3p_\sigma$	$S_{Cys}3p_\pi$	Im
$Cu(Im)_2(SH)(SH_2)^+$: plastocyanin crystal structure									
with SH_2	78	0	1	0	1	0	0	17	1
no SH_2	72	1	0	0	1	0	0	25	1
$Cu(Im)_2(SH)(SH_2)^+$: cucumber basic protein crystal structure									
with SH_2	52	1	15	3	11	2	5	8	1
no SH_2	58	0	10	0	8	2	4	16	2
$Cu(Im)_2(SH)[OCH(NH_2)]^+$: stellacyanin crystal structure									
with $OCH(NH_2)$	59	0	18	3	3	2	3	9	1
no $OCH(NH_2)$	63	0	11	0	3	1	2	19	2

since these transitions originate from the $Cu3d_{xz}$, -$3d_{yz}$, and $3d_{z^2}$ orbitals, respectively, all three of which are interacting (either π or σ) with the axial ligand. In fact, the actual extent of the increase serves as a measure of the strength of this interaction. As could be expected, the largest increase in excitation energy is found for the c ^2A state, originating from the $Cu3d_{z^2}$ orbital, with a σ interaction with the axial ligand. Interestingly, the extent of the effect on the c ^2A state increases within the sequence plastocyanin (1365 cm^{-1}) < cucumber basic protein (2255 cm^{-1}) < stellacyanin (3349 cm^{-1}), indicating an increasing σ interaction with the axial ligand within the series.

It has been suggested by Gewirth et al.[30] that, owing to the strong bond of the axial ligand, a small amount of $3d_{z^2}$ character is mixed into the ground-state orbital of the unpaired electron. They calculated that, in plastocyanin, there is only 0.2% $3d_{z^2}$ mixing in the ground-state singly occupied orbital, whereas in nitrite reductase, where the methionine distance to the copper atom is decreased to 2.59 Å, 1.5% of the ground-state singly occupied orbital consists of $Cu3d_{z^2}$. From the split in the *g* values in the EPR spectrum of stellacyanin, they concluded that in this protein the ground-state singly occupied orbital must have 2−5% of $Cu3d_{z^2}$ character. In Table 6 we have collected the atomic orbital contributions to the ground-state singly occupied orbital of the considered models, with and without the axial ligand. Our calculations confirm Gewirth's suggestion: Table 6 shows that the ground-state orbital of both stellacyanin and cucumber basic protein contains 3% of $Cu3d_{z^2}$ character, while in plastocyanin, this contribution is negligibly small (0.4%). Again, these numbers point to a considerably stronger σ interaction with the axial ligand in both stellacyanin and cucumber basic protein than in plastocyanin. It should be noted however that the interaction is purely ionic in nature: in no case did we find any significant contribution from the axial ligand, either SH_2 or $OCH(NH_2)$, in the singly occupied orbitals of the different states. Moreover the contribution from $3d_{z^2}$ vanishes when the axial ligand, as well as the corresponding σ interaction, is removed (see Table 5).

The most interesting trends are found for the ratios (R_{osc}) between the oscillator strengths of the two charge-transfer bands, f,g ^2A, shown in the last row of Table 5. For the plastocyanin model, removal of the axial ligand leaves R_{osc} unaffected, while in stellacyanin and cucumber basic protein we find a reduction of R_{osc} by about 60%. These numbers are conform with the changes observed in the composition of the ground-state singly occupied orbitals (Table 6). In plastocyanin, the ground-state singly occupied orbital remains almost purely π antibonding, independent of the presence of the fourth ligand. In cucumber basic protein and stellacyanin, on the other hand, removing the fourth ligand and its σ interaction causes a significant shift from σ to π in the ground-state orbital, with the observed shift in R_{osc} as a consequence.

On the whole, it has to be concluded that the differences between the spectra of plastocyanin on one hand and stellacyanin and cucumber basic protein on the other hand must be traced

TABLE 7: CASPT2 Spectra of the Trigonal and Tetragonal Form of $Cu(NH_3)_2(SH)[OCH(NH_2)]^+$ and $Cu(NH_3)_2(SH)(NHCOH)$[a]

state	tetragonal		trigonal		state
C_1	$OCH(NH_2)$	$NHCOH^-$	$NHCOH^-$	$OCH(NH_2)$	C_s
b ^2A	9 839(0.0000]	15 663(0.0002)	1 185(0.0000)	4 046(0.0000)	a $^2A'$
c ^2A	15 538(0.0005)	15 911(0.0000)	8 542(0.0014)	11 292(0.0000)	b $^2A'$
d ^2A	16 655(0.0000)	19 520(0.0002)	10 278(0.0000)	13 217(0.0019)	b $^2A''$
e ^2A	17 078(0.0024)	19 804(0.0000)	13 836(0.0000)	13 630(0.0000)	c $^2A'$
f ^2A	17 000(0.0071)	24 261(0.0007)	12 287(0.1038)	13 230(0.1126)	c $^2A''$
g ^2A	23 360(0.1583)	28 018(0.1346)	19 315(0.0005)	20 453(0.0004)	d $^2A'$

[a] Excitation energies in cm^{-1}; oscillator strengths within parentheses.

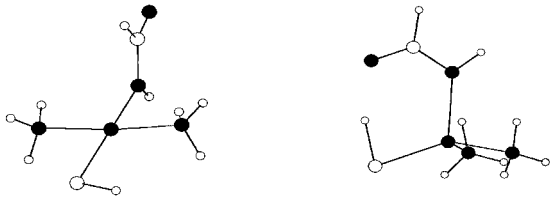

Figure 4. The optimized tetragonal and trigonal structures of the $Cu(NH_3)(SH)(NHCOH)$ model.

back to the same effect, namely a stronger σ interaction with the fourth ligand in the latter proteins. The origin of this σ interaction is different for the two cases. In cucumber basic protein, it is connected to a structural effect (i.e., the tetragonal distortion found in the crystal structure of this protein ($\phi = 70°$)). In the Met121Gln azurin mutant crystal structure, on the other hand, no significant tetragonal distortion is present, and the stronger σ interaction is instead inherent to the glutamine residue with its oxygen instead of sulfur coordinating atom.

6. Does the Coordinating Atom of Glutamine Change at High pH?

The experimental spectrum of stellacyanin and umecyanin change at high pH: the most intense line is blue-shifted from 610 to 580 nm.[4,29,31] This shift is accompanied by changes in the EPR spectrum.[7] It has been suggested[7,12] that this is due to a change of the coordinating atom of the glutamine ligand. At low pH, the O^ϵ atom coordinates to copper. At high pH, the N^ϵ atom might become deprotonated and may then become a good copper ligand. However, this suggestion has lately been challenged.[11] Therefore, we optimized the geometry of $Cu(NH_3)_2(SH)(NHCOH)$ with the nitrogen amide atom as fourth copper ligand. As for the other stellacyanin models, we optimized both a trigonal and tetragonal structure. The two structures are shown in Figure 4, and they are described in Table 1. Interestingly, for these model complexes, the two structures do not have the same energy; the tetragonal structure is 50 kJ/mol more stable than the trigonal structure. In fact, the trigonal structure is not a local minimum, but a transition state. Inspection of the coordinates of the trigonal stucture shows that the $Cu-N_{Gln}$ bond is quite short compared to the $Cu-O_{Gln}$ bond in the $OCH(NH_2)$ models. Consequently, the $Cu-S_{Cys}$ distance increases to 2.19 Å.

In Table 7, the electronic spectra of the trigonal and tetragonal structures of $Cu(NH_3)_2(SH)(NHCOH)$ are compared with the spectra of the corresponding $OCH(NH_2)$ complexes. The trigonal structures exhibit quite similar spectra with a single intense line (c $^2A''$) around 13000 cm^{-1}. However, the tetragonal structures show a single peak around 460 nm (state d $^2A'$) and no intensity around 600 (state c $^2A''$) nm.

Two lines of evidence talk against the suggestion that N^ϵ coordinates to copper at high pH. First, the negatively charged ligand would strongly stabilize the tetragonal structure (by 50 kJ/mol). In the spectrum of the tetragonal structure, the 460 nm peak would be more intense than the peak at 600 nm. Therefore, a strong change in intensity of both peaks would be expected, but is not observed experimentally. Second, even if the protein could stablize the trigonal structure, the calculated spectra show that the blue line would be expected to be red-shifted by the change of the coordinating atom, rather than the observed blue shift.

Since the pH-dependent changes in the absorption spectrum of stellacyanin can occur even in the absence of the glutamine ligand,[32] small structural changes of the copper binding site could influence the $Cu-S_{Cys}$ bond, which is expressed in the spectroscopical shift. Therefore, we must conclude that the coordinating atom of the glutamine ligand does not change at high pH. Instead, we suggest that the spectral shift is caused by a change in the electrostatic field near the copper ion. As can be seen in Table 2, the blue band is very sensitive to the model of the surrounding protein and solvent. A change in the conformation or the charge of the nearby amino acids may easily explain the observed blue shift. For example, Sykes and co-workers have suggested that the shift is caused by the deprotonation of a nearby lysine residue.[29]

Acknowledgment. The authors thank Profs. Albrecht Messerschmidt and Hans Freeman for providing us the coordinates of the Met121Glu azurin mutant and cucumber basic protein before they were available in the Brookhaven Protein Data Bank. This investigation has been supported by grants from the Flemish Science Foundation (FWO), the Concerted Research Action of the Flemish Government, the Swedish Natural Science Research Council (NFR), and by the European Commission through the TMR program (Grant ERBFMRXCT960079). This work was also supported with computer resources by the Leuvens Universitair Dienstencentrum voor Informatica en Telematica (LUDIT), Leuven, and the Swedish Council for High Performance (HPDR), and Parallelldatorcentrum (PDC) at the Royal Institute of Technology, Stockholm.

References and Notes

(1) Sykes, A. G. *Adv. Inorg. Chem.* **1990**, *36*, 377−408.

(2) Adman, E. T. *Adv. Protein Chem.* **1991**, *42*, 145−197.

(3) Holm, R. H.; Kennepohl, P.; Solomon, E. I. *Chem. Rev.* **1996**, *96*, 2239−2314.

(4) Lu, Y.; Lacroix, L. B.; Lowery, M. D.; Solomon, E. I.; Bender, C. J.; Peisach, J.; Roe, J. A.; Gralla, E. B.; Valentine, J. S. *J. Am. Chem. Soc.* **1993**, *115*, 5907.

(5) Ryde, U.; Olsson, M. H. M.; Roos, B. O.; Pierloot, K.; De Kerpel, J. O. A. *Encycl. Comput. Chem.* **1998**. *In press*.

(6) Adman, E. T.; Godden, J. W.; Turley, S. *J. Biol. Chem.* **1995**, *270*, 27458−27474.

(7) Peisach, J.; Levine, W. G.; Blumberg, W. E. *J. Biol. Chem.* **1967**, *242*, 2847.

(8) Obokata, J.; Mikami, K.; Hayashida, N.; Nakamura, M.; Sugiura, M. *Plant Physiol.* **1993**, *102*, 1259.

(9) Romero, A.; Hoitink, C. W. G.; Nar, H.; Huber, R.; Messerschmidt, A.; Canters, G. W. *J. Mol. Biol.* **1993**, *229*, 1007.

(10) Hart, P. J.; Nersissian, A. M.; Herrmann, R. G.; Nalbandyan, R. M.; Valentine, J. S.; Eisenberg, D. *Protein Sci.* **1996**, *5*, 2175.

(11) Nersissian, A. M.; Mehrabian, Z. B.; Nalbandyan, R. M.; Hart, P. J.; Fraczkiewicz, G.; Crernuszewicz, R. S.; Bender, C. J.; Peisach, J.; Hermann, R. G.; Valentine, J. S. *Phys. Scri.* **1996**, *5*, 2184.

(12) Fields, B. A.; Guss, J. M.; Freeman, H. C. *J. Mol. Biol.* **1991**, *222*, 1053−1065.

(13) Ryde, U.; Olsson, M. H. M.; Pierloot, K.; Roos, B. O. *J. Mol. Biol.* **1996**, *261*, 586−596.

(14) Pierloot, K.; De Kerpel, J. O. A.; Ryde, U.; Roos, B. O. *J. Am. Chem. Soc.* **1997**, *119*, 218−226.

(15) Olsson, M. H. M.; Ryde, U.; Roos, B. O.; Pierloot, K. *J. Biol. Inorg. Chem.* **1998**, *3*. In press.

(16) Rice, J. E.; Horn, H.; Lengsfiels, B. H.; McLean, A. D.; Carter, J. T.; Replogle, E. S.; Barnes, L. A.; Maluendes, S. A.; Lie, G. C.; Gutwski, M.; Rude, W. E.; Sauer, S. P. A.; Lindh, R.; Andersson, K.; Chevalier, T. S.; Widmark, P.-O.; Bouzida, D.; Pacansky, G.; Singh, K.; Gillan, C. J.; Carnevali, P.; Swope, W. C.; Liu, B. *Mulliken*, Version 2.31h (internal release); IBM Corporation; Almaden, 1995.

(17) Frisch, M. J.; Trucks, G. W.; Schlegel, H. B.; Gill, P. M. W.; Johnson, B. G.; Robb, M. A.; Cheeseman, J. R.; Keith, T.; Petersson, G. A.; Montgomery, J. A.; Raghavachari, K.; Al-Laham, M. A.; Zakrzewski, V. G.; Ortiz, J. V.; Foresman, J. B.; Cioslowski, J.; Stefanov, B. B.; Nanayakkara, A.; Challacombe, M.; Peng, C. Y.; Ayala, P. Y.; Chen, W.; Wong, M. W.; Andres, J. L.; Replogle, E. S.; Gomperts, R.; Martin, R. L.; Fox, D. J.; Binkley, J. S.; Defrees, D. J.; Baker, J.; Stewart, J. P.; Head-Gordon, M.; Gonzalez, C.; Pople, J. A. *Gaussian 94*, Revision D.1; Gaussian, Inc.: Pittsburgh, PA, 1995.

(18) Ricca, A.; Bauschlicher, C. W. *J. Phys. Chem.* **1994**, *98*, 12899−12903.

(19) Schäfer, A.; Horn, H.; Aldrichs, R. *J. Chem. Phys.* **1992**, *97*, 2571−2577.

(20) Roos, B. O.; Andersson, K.; Fülscher, M. P.; Malmqvist, P.-Å.; Serrano-Andrés, L.; Pierloot, K.; Merchán, M. In *Advances in Chemical Physics: New Methods in Computational Quantum Mechanics*; Vol. XCIII Prigogine, I., Rice, S. A., Eds. John Wiley & Sons: New York, 1996; p 219.

(21) Pierloot, K.; Dumez, B.; Widmark, P.-O.; Roos, B. O. *Theor. Chim. Acta* **1995**, *90*, 87.

(22) Malmqvist, P. Å.; Roos, B. O. *Chem. Phys. Lett.* **1989**, *155*, 189.

(23) Andersson, K.; Fülscher, M. P.; Karlström, G.; Lindh, R.; Malmqvist, P.-Å.; Olsen, J.; Roos, B. O.; Sadlej, A. J.; Blomberg, M. R. A.; Siegbahn, P. E. M.; Kellö, V.; Noga, J.; Urban, M.; Widmark, P.-O. *MOLCAS*, Version 3; Department of Theoretical Chemistry, Chemistry Center, Lund University: Lund, 1994.

(24) Cornell, W. D.; Cieplak, P.; Bayly, C. I.; Gould, I. R.; Merz, K. M.; Ferguson, D. M.; Spellmeyer, D. C.; Fox, T.; Caldwell, J. W.; Kollman, P. A. *J. Am. Chem. Soc.* **1995**, *117*, 5179−5197.

(25) Pearlman, D. A.; Case, D. A.; Caldwell, J. W.; Ross, W. S.; Cheatham, T. E.; Ferguson, D. M.; Seibel, G. L.; Singh, U. C.; Weiner, P. K.; Kollman, P. A. *Amber*, Version 4.1; University of California: San Francisco, 1995.

(26) Malmström, B. G. *Eur. J. Biochem.* **1994**, *223*, 207−216.

(27) Williams, R. J. P. *Eur. J. Biochem.* **1995**, *234*, 363−381.

(28) Guss, J. M.; Bartunik, H. D.; Freeman, H. C. *Acta Crystallogr.* **1992**, *B48*, 790−807.

(29) Dennison, C.; Van Driessche, G.; Van Beeumen, J.; McFarlane, W.; Sykes, A. G. *Chem. Eur. J.* **1996**, *2*, 104−109.

(30) Gewirth, A. A.; Cohen, S. L.; Schugar, H. J.; Solomon, E. I. *Inorg. Chem.* **1987**, *26*, 1133−1146.

(31) Thomann, H.; Bernardo, M.; Baldwin, M. J.; Lowery, M. D.; Solomon, E. I. *J. Am. Chem. Soc.* **1991**, *113*.

(32) Fraczkiewicz, G.; Nersissian, A. R.; Hart, J. P.; Valentine, J. S.; Czernuszewicz, R. S. *J. Inorg. Biochem.* **1997**, *67*, 49.